# The art of taming light: ultra-slow and stopped light

*Zachary Dutton[1,2], Naomi S. Ginsberg[2], Christopher Slowe[2], and Lene Vestergaard Hau[2]*
*[1] Lyman Laboratory, Harvard University, Cambridge MA 02138*
*[2] Present address: National Institute of Standards and Technology, Electron and Optical Division, Gaithersburg MD 20899-8410*

In 1998, laser pulses were slowed [1] in a Bose-Einstein condensate (BEC) [2] of sodium to only 17 m/s, more than seven orders of magnitude lower than the speed of light in vacuum. Associated with the dramatic reduction factor for the light speed was a spatial compression of the pulses by the same large factor. A light pulse, which was more than 1 km long in vacuum, was compressed to a size of ~50 μm, and at that point was completely contained within the condensate [1]. This allowed the light-slowing experiments to be brought to their ultimate extreme [3]: in the summer of 2000, light pulses were completely stopped, stored, and subsequently revived in an atomic medium, with millisecond storage times [4]. The initial ultra-slow light experiments spurred a flurry of slow light investigations, and slow or partially stopped light has now been observed in limited geometries in warm rubidium vapours [5-7], liquid-nitrogen cooled crystals [8], and recently in room temperature crystals [9].

Here, we begin with a discussion of ultra-slow and stopped light. We describe how cold atoms and Bose-Einstein condensates have been manipulated to generate media with extreme optical properties. While the initial experiments concentrated on the light propagation, we have recently begun a number of investigations of the effects that slow light has on the medium in which it propagates. Effects are profound because both the velocity and length scales associated with propagating light pulses have been brought down to match the characteristic velocity and length scales of the medium. With the most recent extension, the *light roadblock* [10], we have compressed light pulses to a length of only 2 μm. Here, we describe the use of ultra-compressed light pulses to probe superfluidity and the creation of quantized vortices in BECs through formation of 'superfluid shock waves'.

We also present the observation of an ultra-slow-light-based, pulsed atom laser. Furthermore, we demonstrate the use of slow and stopped light for manipulation of optical information, in particular in Bose-Einstein condensates that allow for phase coherent processing of three-dimensional, compressed patterns of stored optical information.

## Ultra-slow light

In our experiments we use a cloud of ultra-cold sodium atoms, trapped by an electromagnet in an ultra-high vacuum chamber (Fig. 1a). By illuminating the cloud with a precisely tuned 'coupling' laser beam, the optical properties of the atoms can be dramatically altered so that a laser pulse, subsequently sent through this coupled atom-light medium, will move at very low velocity. By choosing the right polarisations of the two laser beams, the light fields selectively couple three internal energy levels of the atoms (Fig 1b).

Initially, the atoms are all in the ground state labeled $|1\rangle$, and the laser fields are off. The coupling laser is turned on and couples $|2\rangle$ to the upper state, $|3\rangle$. Since $|2\rangle$ is unpopulated, the coupling laser is not absorbed but rather causes the upper energy level, $|3\rangle$, to split symmetrically into two new energy levels (Fig. 1b). The energy difference between these new states is proportional to the magnitude of the electric field of the coupling laser. A 'probe' light pulse, tuned to the $|1\rangle$-$|3\rangle$ transition, is injected into the BEC. It is this light pulse that is compressed and propagates at ultra low group velocity. A light detector (PMT in Fig. 1a) is used to measure the arrival of the pulse as it exits the atom cloud.

The refractive index profile for the probe pulse in the slow-light medium is shown in Fig 1c. The refractive index on resonance is unity—the value in free space—because the contributions to the susceptibility from the two symmetrically split energy levels exactly cancel. This results in a steep and linear refractive index variation around the $|1\rangle$-$|3\rangle$ resonance, which leads to low light speeds since the signal velocity of a light pulse is inversely proportional to the refractive index *slope*. With cold atoms there is a negligible Doppler smearing of the energy levels and illumination with very low coupling intensities is possible. This brings the split levels close together and creates very steep refractive index slopes and extremely low light speeds. While the pulse is in the atom cloud, its group velocity and spatial extent are both proportional to the intensity of the coupling field and inversely proportional to the atom density. These parameters can be experimentally controlled.

A resonant probe pulse would be completely attenuated in the atom cloud in the absence of the coupling laser. However, when the coupling laser is present, a narrow transmission window is created around resonance, and the pulses can propagate though the atom cloud. This effect, electromagnetically induced transparency [11], is also responsible for maintaining the very steep slopes of the refractive index profile, even in the presence of spontaneous radiation damping from the upper state, $|3\rangle$, which would otherwise broaden the profile in Fig. 1c. It occurs due to a quantum mechanical interference created in the atom-light system: absorption of a probe photon is associated with the transition of an atom from $|1\rangle$ to $|3\rangle$. However, there is another path to that final state, where the atom absorbs a coupling photon and makes a transition from $|2\rangle$ to $|3\rangle$. As a result, when the atom is in a very particular quantum mechanical superposition of $|1\rangle$ and $|2\rangle$, the transition amplitudes for the two paths cancel. In this 'dark state', the atom absorbs from neither the probe nor the coupling laser fields, and the amplitude for the atom to be in $|2\rangle$ relative to the amplitude for $|1\rangle$, $A_2/A_1$, is proportional to minus the ratio of the electric field amplitudes of the probe and coupling laser fields. This makes the process phase sensitive: the ratio $A_2/A_1$ is a complex number that depends on the relative phase of the probe and coupling fields.

As the light pulse enters the atom cloud, the front edge slows down, the back edge—still in free space—catches up and the pulse spatially compresses. As the pulse propagates through the atom cloud, the atoms within the spatially localized pulse region are in dark superposition states. The spatial distribution of the dark states mimics the spatial variation of the light pulse: the pulse makes an imprint—a hologram, really—in the atom cloud and this imprint follows the pulse as it slowly propagates. Eventually the light pulse and the imprint reach the other end of the cloud where the front edge speeds up and the pulse expands spatially. The light pulse reaches the same shape as it had before it entered the medium, but is delayed by several microseconds in a cloud of only 100-200 μm (Fig 1d).

Fig. 2a shows images of the atomic imprint of a 2 μs light pulse, with a length of 600 m in free space, as it compresses and propagates into a 100 μm long and 30 μm wide, cigar-shaped

Bose-Einstein condensate. To photograph the pulse, we selectively image $|2\rangle$ atoms in the cloud with the 'imaging' laser beam shown in Fig.1a, revealing the instantaneous shape of the imprint. The transverse width of the probe laser beam (in the *x*-*y* plane) is larger than the size of the condensate. The pulse is entering the cloud, and compressing, through the first 5 μs and then starts its slow propagation into the cloud. The observed boomerang shape of the light pulse (at 5 μs) reflects that the light speed along the centreline of the condensate is significantly lower than at the edges due to the high atom density in the middle of the cloud.

## Stopped light

Because of the aforementioned spatial compression, the light pulse is eventually completely contained within the atom cloud. By an abrupt turn-off of the coupling laser, the moving light pulse stops and turns off, but leaves the holographic imprint frozen in the cloud [4]. Figure 2b shows a light-stopping experiment performed in a Bose-Einstein condensate, with two probe light pulses incident on the condensate from opposite directions. The light pulses are stopped in the atom cloud just before they collide, resulting in an imprint with a double boomerang shape (0 ms). Because of photon-induced recoils, that come from the coherent transfer of atoms from $|1\rangle$ to $|2\rangle$, the two 'boomerangs' are shot out at ± 45°, each with a velocity of 4.2 cm/s. This shows very directly that the process is coherent: to reach $|2\rangle$, the atoms absorb a probe photon and emit a coupling photon through *stimulated* emission. If instead, $|2\rangle$ had been reached via spontaneous, incoherent emission from $|3\rangle$, the two ejected atom clouds would (on average) have been kicked out along the ±*z*-directions and would have had a velocity spread comparable to the recoil velocity.

Since the slow-light and light-storage process is coherent, the ejected imprints are small condensates of $|2\rangle$ atoms. The observed changes in shape of the imprints as a function of time, as shown in Fig 2b, are indeed in agreement with calculations of condensate dynamics, based upon mean-field theory [12]. In effect, we have created a pulsed atom laser with a controllable spatial mode and a well-defined output-coupling velocity. Such an ultra-slow-light-based atom laser could be used as a source for a high-brightness atom interferometer. Such interferometers are beginning to rival classical precision measuring devices including navigational gyroscopes [13] and gravitometers [14].

We have also studied the case of stopped light for co-propagating coupling and probe laser beams with opposite circular polarisations. In this case, photon-recoil effects are negligible, and atoms in $|2\rangle$ are trapped by the electromagnet similarly to atoms in $|1\rangle$. The holographic imprint of the stopped light pulse therefore stays in the cloud for a long time. By switching the coupling field back on, the amplitude and phase of the atomic wavefunctions are written back onto the probe field, and the light pulse is revived after a long storage time in the medium.

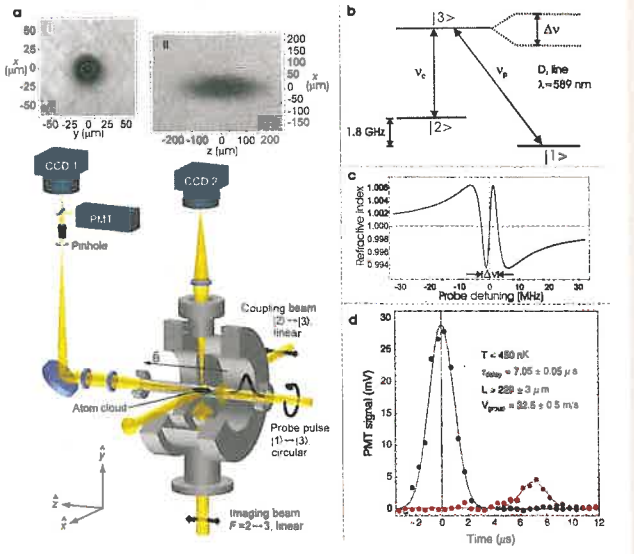


▲ **Fig. 1: Ultra-Slow Light**

**(a)** Experimental setup for generating slow and stopped light (from ref. 1). The cigar-shaped, cooled atom cloud, consisting of sodium atoms in state $|1\rangle$ (see (b)), is typically 100-200 μm long and is trapped in an electromagnet. The cloud is first illuminated from the side (along *x*) by a coupling laser beam. The intensity and frequency of this illuminating laser control the optical properties—in particular, the refractive index profile and the transmission—for a probe laser pulse subsequently sent into the medium (along *z*). This light pulse then propagates extremely slowly through the atom cloud. For propagation in a BEC, we obtain, with low coupling laser power (12 mW/cm²), a light speed of only 17m/s. The condensate would be completely opaque in the absence of the coupling field, but the presence of this laser field allows transmission of the light pulse (electromagnetically induced transparency). A photo-multiplier tube (PMT) is used to measure the delay and transmission of a probe pulse. The size of the atom cloud is determined with use of a third laser, the 'imaging beam'. This laser beam is sent into the system from below (along *y*) and the absorption shadow of the atom cloud, created in the beam, is recorded on a CCD camera (CCD2). An example is shown in inset (ii). Another camera, CCD1, is used to image the cloud in the x-y plane. For the slow and stopped light experiments (Figs 1 and 3), a pinhole is placed in an external image plane so the PMT detects light only that has been transmitted through the central 15 microns of the condensate (indicated by the dashed circle in insert (i)).

**(b)** Three-level (Λ) system of internal atomic states used to create slow light. The probe and coupling laser beams are resonant with the $|1\rangle$-$|3\rangle$ and $|2\rangle$-$|3\rangle$ transitions, respectively, and couple the three states. Here, $\nu_p$ and $\nu_c$ represent the resonance frequencies, and Δν is the distance between the new split energy levels of the atom/coupling-laser medium. Through the choice of frequencies and polarisations for the probe and coupling lasers, we control which atomic states participate in the process. The states used for the ultra-slow light measurement in (d), obtained with the polarisations indicated in (a), are $|1\rangle=|3S,F=1,M_F=-1\rangle$, $|2\rangle=|3S,F=2,M_F=-2\rangle$, and $|3\rangle=|3P_{3/2},F=2,M_F=-2\rangle$.

**(c)** Refractive index profile. We show the refractive index for the probe laser as a function of its detuning from the $|1\rangle$-$|3\rangle$ resonance frequency. Note that the refractive index on resonance is unity, the value in free space. Importantly, the refractive index has a very steep slope around resonance, and since the group velocity of a light pulse is inversely proportional to that slope, the profile shown leads to ultra-slow light. The figure was obtained for a coupling intensity of 12 mW/cm² and an atomic density of $3.3\cdot10^{12}$/cm³.

**(d)** Observation of ultra-slow light (ref. 1). The blue data points represent a reference pulse recorded with no atoms in the system and used to set the zero-point for the time axis. The red data points show a pulse that has propagated through an atom cloud cooled to 450 nK which is just above the transition temperature for BEC (the peak atomic density, in the cloud centre, is $3.3\cdot10^{12}$/cm³). In this case the delay of the light pulse is 7 μs, in a cloud that is only 229 μm long (see insert (ii) in (a)). This results in a light speed of 32 m/s which is seven orders of magnitude below the value in free space.

Fig. 3a shows a slow-light measurement with this setup, performed in a cold atom cloud cooled to 900 nK (which is just above the transition temperature for Bose-Einstein condensation). The pulse delay is 12 μs, and the arrow indicates the point in time when the light pulse is slowed, compressed, and totally contained in the middle of the atom cloud. In Figs 3b-c we abruptly turn the coupling laser off at this time and freeze a holographic imprint in the cloud. Since the imprint contains all the amplitude and phase information of the original light pulse, we can later revive the light pulse and send it back on its way, by simply turning the coupling laser back on. The storage times for the light pulse are 38 μs (Fig. 3b) and 833 μs (Fig. 3c), respectively.

The revived light pulses can also be manipulated [4]. In Figs 3d-e, a single light pulse is stored in the atom cloud and later regenerated in two (Fig. 3d), and even three, small pieces (Fig. 3e) by switching the coupling laser on and off several times. Furthermore, we have observed that by turning the coupling laser back on at a higher (lower) intensity, a temporally shorter (longer) light pulse can be regenerated. In the language of optical engineering, the bandwidth of the system can be manipulated dynamically, even for Fourier transform limited pulse propagation.

The storage times for compressed optical information are limited due to thermal smearing of the stored imprints, and are optimised with the ultra-cold clouds we are using. For the parameters in Figs 3, the storage time was limited to a few milliseconds.

## Coherent processing of optical information

This storage time can be increased dramatically with optical storage in Bose-Einstein condensates, which are phase coherent objects. Furthermore, the dynamics of the condensates during the storage time can be utilised for processing of the stored optical information. The dynamics change the spatial structure of the ground state coherences—the dark states—leading to regenerated probe pulses with amplitude and phase changes that reflect the dynamics.

We have developed a comprehensive formalism to study these effects [15,16] and examples are shown in Fig. 4. Storing a slowed light pulse in a BEC creates a two-component condensate, a mixture of $|1\rangle$ and $|2\rangle$ atoms. The ensuing dynamics include nonlinear atom-atom interactions between the two condensate components. Our formalism, based on self-consistent Maxwell and condensate mean-field equations, describes a two-component BEC exposed to coupling and probe laser fields.

In Fig. 4a, the condensate component of $|1\rangle$ atoms creates a mean-field repulsive potential for the component of $|2\rangle$ atoms. The sum of the magnetic trapping potential and this mean field forms an effective potential with sharp edges. The $|2\rangle$ condensate reflects off this boundary, which leads to formation of interference fringes in the density of $|2\rangle$ atoms. Remarkably, by subsequent turn-on of the coupling laser, these complicated structures are written, with high fidelity, onto a revived probe pulse (Fig. 4b).

Unlike the above example, which utilises a weak probe field, a different regime is represented by Figs 4c-d where a strong probe pulse, of about the same peak electric field amplitude as that of the coupling field, propagates into a condensate and is stored (Fig. 4c). In this case, the slow-light and storage process significantly changes the density of both condensate components, and this leads to strong nonlinearities in the condensate dynamics. In Fig. 4d (left), the two components are seen to phase-separate, and two dark solitons are spontaneously formed in the condensate of $|1\rangle$ atoms, with

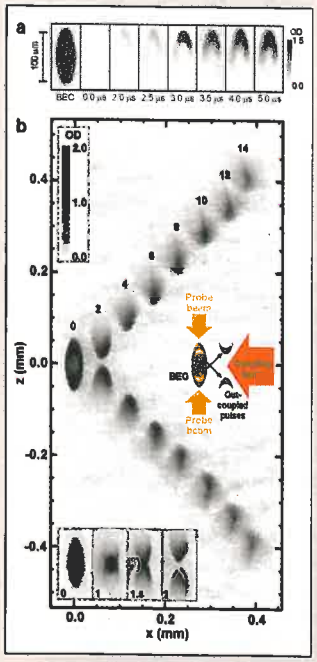


▶ **Fig. 2: Atom Laser with Ultra-Slow and Stopped Light**
**(a)** Observation of the slow-down and spatial compression of a light pulse in a BEC. Setup is as in Fig 1a. The first figure ('BEC') shows a condensate of $|1\rangle$ atoms, imaged before the light pulse is sent in. The picture is taken with the imaging beam and recorded on CCD2. The condensate is subsequently illuminated with the coupling laser and the probe light pulse is sent into the atom cloud. As described in the text, within the light pulse region, the atoms are in coherent dark states that are superpositions of $|1\rangle$ and $|2\rangle$. The spatial distribution of the dark states mimics the spatial shape of the light pulse. This atomic imprint, created by the light fields, travels with the light pulse. By selectively imaging the density of atoms in $|2\rangle$ (on CCD2), we can thus image the light pulse as it propagates through the condensate. The following pictures (from 0 μs to 5 μs) show such images of the light pulse as it propagates into the atom cloud and spatially compresses. At 0 μs, we start inputting the front edge of the light pulse. After 5 μs, the pulse is fully input, compressed, and totally contained within the cloud. The pulse starts out in free space, with a Gaussian shape and a length of 1 km, and is compressed in the condensate to only 25 μm. The light pulse is also seen to develop a 'boomerang' shape. The probe laser beam is uniform across the cloud in the *x*-direction (in the *y*-direction, the beam is only 20 μm wide to minimize smearing of the pulse shape in the images), and in the middle of the condensate, where the atom density is high, the pulse travels significantly slower than at the edge of the cloud, where the density is low, creating the boomerang shape. The grey-scale indicates the on-resonance optical density (OD) of the images, obtained as minus the natural logarithms of the transmission coefficient.
**(b)** Atom laser. For this experiment we send two counter-propagating probe light pulses into a Bose-Einstein condensate where they are stopped and form the double-boomerang imprint in the cloud labeled '0'. (The numbers in the figure indicate the times, in milliseconds, after the light pulses are input and stopped). Again, we selectively image the density of $|2\rangle$ atoms. To reach $|2\rangle$, the atoms have absorbed a probe photon and, through stimulated emission, emitted a coupling photon, leading to a $\pm 45°$ photon-induced recoil of the $|2\rangle$ atoms. We clearly see the two recoiling, boomerang-shaped imprints of $|2\rangle$ atoms as they are kicked out of the condensate (2-14 ms) with a velocity of 4.2 cm/s. They cross at 1 ms as shown in the inset. At 2 ms, the imprints are separated again but still maintain their boomerang shape. Since the slow-light and storage process is fully coherent (as confirmed by the recoil directions), and the atom imprints are output-coupled from a condensate, the ejected atom clouds are condensates of $|2\rangle$ atoms. This is confirmed by studying the ensuing dynamics. The associated shape changes as a function of time agree with a Gross-Pitaevskii mean-field description [12] of condensate dynamics. Between the boomerang arms, a narrow 'snout' of atoms forms, which is clearly seen sticking upward (on the upper track) at 10 and 12 ms. This sharp feature is due to an interference between atoms moving inward from the two boomerang arms. With this setup, we have created a pulsed atom laser with spatially controlled output coupling. In the case shown, there are 5 million atoms in the initial condensate of $|1\rangle$ atoms, and each output coupled condensate of $|2\rangle$ atoms contain 225,000 atoms.

the associated density dips filled by $|2\rangle$ atoms. (Solitons are excitations that maintain their shape due to a perfect balance between dispersion of collective excitations and nonlinear atom-atom interactions. Dark solitons give rise to a depletion of the atom density [17] as opposed to bright solitons where the density is enhanced). The result is extremely stable, filled 'vector solitons' [18,19]. Due to phase gradients in the condensate, the vector solitons move around and interact with each other. Upon subsequent pulse revival, the relative amplitude and phase of the two-component condensate, including the solitons, are written onto and transferred to the light fields (Fig 4d, right panel). We see that in this strong probe case, the coupling light field is also strongly affected by the atom dynamics.

It is now clear that by controlling the coupling beam parameters, the shape and size of the outgoing probe pulses can be manipulated, and mapping between atomic and light media can be performed with high fidelity [15]. In the weak-probe limit and for certain atom-atom interaction parameters, the $|2\rangle$ atoms experience, during the storage time, a predictable trapping potential with its own set of eigenstates. By choosing an incoming probe pulse profile that corresponds to one of these eigenstates, the amplitude of the stored imprint is stationary, and the imprint will evolve purely in phase. This setup could form the basis for a one-bit phase shifting gate. If the initial pulse is not a pure eigenstate of the system, as in Fig. 4a, it can be represented by a superposition of eigenstates that will evolve independently and lead to deterministic reshaping of the revived light pulse. Inputting stronger probe pulses leads to nonlinear evolution in the condensate which can be used for nonlinear processing of pulses. For example, one could input two spatially separated light pulses and the ensuing evolution will cause them to interact and introduce additional phase shifts on each other. This is the ingredient necessary to construct a two-bit conditional phase gate—a fundamental building block of quantum (or optical) computation. Furthermore, atom-atom interactions can be controlled with external electric and magnetic fields [20,21], with the exciting potential for dynamically controlled processing of stored optical information.

Following the storage of a classical light pulse in a BEC, condensate dynamics could develop non-classical entangled-atom states [22,23]. By subsequently reviving the light pulse [24], we could generate non-classical light fields from purely classical input fields. The storage and revival of non-classical light fields, with controlled processing during the storage time, as described above, could be of great importance for quantum information processing where the transfer between flying qubits (photons for example) and stationary storage devices (atoms for example) is of paramount importance [25].

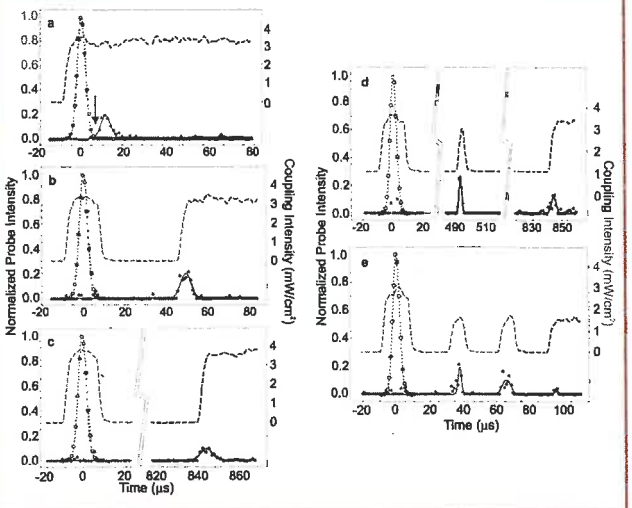


**▲ Fig. 3: Stopped Light**

**(a)** Slow light pulse observed as in Fig. 1d. However, in this case, the probe and coupling lasers are co-propagating and have opposite circular polarisations. The Λ system here has $|2\rangle=|3S,F=2,M_F=+1\rangle$ and $|3\rangle=|3P_{1/2},F=2,M_F=0\rangle$. There is no photon recoil and both $|1\rangle$ and $|2\rangle$ are trapped by the magnet ($|1\rangle$ and $|2\rangle$ have opposite gyromagnetic ratios). In the figure, open circles represent a measured reference pulse, and solid dots represent a pulse measured after it has been delayed by 12 μs in a cold cloud (900 nK with peak density $10^{13}/cm^3$). The dashed curve shows the intensity of the coupling laser which is turned on just a few microseconds before the probe pulse is sent in. The arrow indicates the point in time when the pulse is slowed, compressed, and contained in the middle of the cloud.

**(b-c)** Observation of stopped light. At the point in time indicated by the arrow in (a), we abruptly turn off the coupling laser, with the result that no probe pulse emerges. Some 38 μs later (b), we turn the coupling laser back on, and a light pulse is observed, with the same shape and intensity as measured in (a). Clearly, in this case, we have stopped the pulse and later revived it. In (c) we perform the same experiment as in (b) except we store the imprint in the cloud for 833 μs before we revive the light pulse.

**(d-e)** Manipulation of stored optical information. Here we inject and stop a single light pulse in the atom cloud. By switching the coupling laser on and off several times, we regenerate the light pulse in two small pieces (d) and even in three small pieces (e). The probe pulse intensity in the figures is normalised to the peak intensity of the reference pulse. Figs (a-e) are from ref. 4.

## The light roadblock and superfluid dynamics

We now turn our attention to the description of how slow light can be used for direct probing of superfluid properties of Bose-Einstein condensates. By spatial modulation of the coupling laser intensity along the propagation direction of the probe pulses [10], we can, for example, control the speed and spatial extent of light pulses as they are propagating through the atom cloud. By spatially cutting off the coupling laser in the middle of the condensate, we form a *light roadblock*: a probe pulse slows down and compresses dramatically as it is running into the region of very low coupling intensity (Fig. 5a). With this method, light pulses 1 km-long in free space are compressed to 2 μm in a Bose-Einstein condensate. Within the localised pulse region at the roadblock, the atoms are driven almost entirely into $|2\rangle$ (the dark state when the coupling intensity goes to zero). As discussed above (Fig. 2b), the localised 'defect' of $|2\rangle$ atoms is kicked out of the magnet in less than a millisecond, due to photon recoil.

In the electromagnet, we are thus left with a $|1\rangle$-atom condensate with a slice punched in the middle. This void is so localised that it is comparable to the condensate's healing length, the length over which a superfluid can adjust to external perturbations [26]. The density depletion of the condensate breaks into two density dips that move at the local sound speed towards the condensate boundaries. Since the density defects are narrow and deep, nonlinearities from atom-atom interactions lead to a steepening of their back edges during propagation in the condensate, which results in 'quantum shock waves' [10], the superfluid analogue of shock waves in a classical fluid.

An experimental observation of this process is shown in Fig. 5b (from ref. 10). A narrow density defect is created at the light roadblock, which immediately leads to formation of dark solitons (white stripes at 0 ms). However, the solitons are unstable and their fronts

start to curl up, as seen at 0.5 ms. Subsequently, the points along the main front, with the largest curvature, act as nucleation sites for vortices with quantized circulation [26]. Vortices are observed at 2.5 ms and are seen as white 'dots' where the condensate density vanishes. Quantized vortices are very stable excitations of the superfluid condensate. They are clearly seen at 11 ms, for example.

By means of shock-wave formation, vortices are created far out of equilibrium, in pairs of opposite circulation, like particle anti-particle pairs. Changing the length and intensity of a light pulse sent towards the light roadblock adjusts the number of vortices formed. Hence, we can controllably form many-body systems of vortices and study their collision dynamics: in some cases the vortices collide like billiard balls, in other cases their collisions lead to annihilation and the energy is released in the form of outgoing sound waves.

An example is shown in Fig. 6a, which is the result of a numerical simulation of vortex dynamics in two dimensions, for realistic experimental parameters. After a narrow defect is created at the light roadblock, a total of 12 vortices are nucleated (11 ms). Examination of the phase pattern of the condensate wavefunction reveals that the vortices are singly quantized. They are created in pairs of opposite circulation, with each vortex pair located at opposite sides of the horizontal symmetry axis ($x=0$). The three vortices in each quadrant spin around each other due to the velocity fields of adjacent vortices, two out of each triplet annihilate, and the energy is carried off as sound waves (seen as curved fronts at 16.5 ms and 17.5 ms).

There are then four long-lived vortices remaining. The vortices first move towards the condensate edge, scatter, and circle back towards the centre, which puts them on a collision course. At 57 ms they collide and their paths make a sharp 90° turn. The vortices then circle back after colliding with the condensate boundaries, and a second collision occurs after 122 ms, which gives rise to a sound wave (the curved fronts at 123 ms) that is seen emanating from the centre.

We should be able to create a controlled many body system of these 'vortex particles' as illustrated by the calculation shown in Fig. 6b. Here, a light pulse, stopped at a light roadblock in a pancake shaped BEC, causes a whole line of vortices to form on both sides of the condensate. With the addition of a third dimension, vortex rings and filaments replace these vortex point particles and introduce a

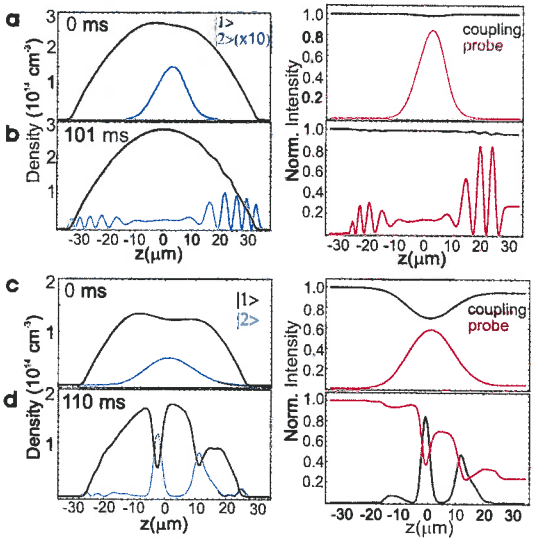


**▲ Fig. 4: Coherent Processing of Optical Information**
The calculations are performed for $^{87}$Rb (note that all other figures are for sodium). Rubidium has scattering rates, for inelastic scattering between the hyperfine ground states $|1\rangle$ and $|2\rangle$ (of the $\Lambda$ system), that are lower than those in sodium by two orders of magnitude [30]. Rubidium is therefore particularly well suited for coherent processing over long time scales.
**(a-b)** Weak probe case. A probe pulse is injected into a BEC under ultra-slow-light conditions and subsequently stopped in the condensate (at 0 ms). The corresponding densities of $|1\rangle$ (black) and $|2\rangle$ (blue) condensate atoms are shown in the left panel of (a). Coherent two-component condensate dynamics, with atom-atom interactions playing a major role, will effectively process the stored light pulse information. In the example shown here, the condensate component of $|2\rangle$ atoms will scatter off the sharp potential edge formed by the magnetic trapping potential in combination with the repulsive mean-field potential from the $|1\rangle$ component. The reflected condensate component interferes with itself and forms interference fringes in the density of $|2\rangle$ atoms (b). The right panels show the results of switching the coupling laser back on at 0 ms and at 101 ms, respectively. Remarkably, the complicated interference pattern in the $|2\rangle$ condensate is written onto the probe light field with high fidelity (the red curve represents the probe intensity normalised to the peak intensity of the input pulse). The coupling intensity (normalised to the input intensity and shown as the black curve) is hardly affected.
We use co-propagating probe and coupling laser beams with opposite circular polarisations such that the states forming the $\Lambda$ system are $|1\rangle=|5S,F=2,M_F=+1\rangle$, $|2\rangle=|5S,F=1,M_F=-1\rangle$, and $|3\rangle=|5P_{1/2},F=2,M_F=0\rangle$. Dictating this choice was our desire for a particular relationship between the scattering strengths for the different condensate components, which control the processing. Here, the s-wave scattering length for collisions between $|2\rangle$ atoms is $a_{22}=5.36$ nm, and the ratios between this quantity and the scattering lengths for collisions between $|1\rangle$ atoms and between $|1\rangle$ and $|2\rangle$ atoms are $a_{11}:a_{12}:a_{22}=0.95:0.975:1$. There is no photon-induced recoil, and both condensate components are trapped by the magnet.
**(c-d)** Strong probe case. This represents a different regime, where the probe and coupling laser strengths are comparable. This leads to significant nonlinear effects in the condensate dynamics, and associated nonlinear processing of optical information is possible. When a probe light pulse is input and stopped in the condensate (0 ms), a large fraction of the atoms within the pulse region are transferred to $|2\rangle$. The corresponding depletion of the condensate of $|1\rangle$ atoms is significant and influences the ensuing two-component condensate dynamics, leading to the nonlinearities. In this case, the two components phase-separate: the $|1\rangle$-condensate component develops two dark solitons filled with state $|2\rangle$ condensate atoms. The resulting density in the two components, after 110 ms of evolution, is shown in (d), left panel. The coupling laser is switched on at this time, and the revived probe pulse is shown in the right panel (red curve). As is seen, the solitons are written onto the probe light field. In this strong-probe case, the coupling laser is significantly affected by the write process, and it is really in the ratio of the two light field amplitudes that the full result of the processing is contained. The solitons correspond to large phase gradients in the condensate wavefunction, and these phase gradients are also written onto the light fields [15].
For these calculations, we used co-propagating probe and coupling laser beams with opposite circular polarisations, but now with frequencies of the laser fields tuned such that the states of the $\Lambda$ system are $|1\rangle=|5S,F=1,M_F=-1\rangle$, $|2\rangle=|5S,F=1,M_F=+1\rangle$, and $|3\rangle=|5P_{1/2},F=2,M_F=0\rangle$. The scattering lengths are $a_{11}=a_{22}=5.36$ nm, and $a_{12}=1.04\,a_{11}$. The latter is larger than the value for an isolated rubidium atom where $a_{12}=1.005\,a_{11}$. The larger value is chosen in order to speed up the processing. Scattering lengths can be controlled with external electric and magnetic fields.

host of new and exciting dynamics as a result of the more complicated topology.

Spatial modulation of the coupling laser [10] in a slow light medium forms the basis for the proposed observation of effects of general relativity in table-top, earth-based experiments [27], and for recent photonic bandgap induced storage of light pulses in atomic media [28].

## Outlook

As described above, ultra-slow light allows for the ultimate control of light: the manipulation, storage, and processing of optical information. We imagine that ultra-slow light can be used as a basis for creating dynamically controllable optical delay lines with large and variable optical delays obtained in very small optical structures. The delays and the bandwidth of such a system could be controlled simply through control of the coupling laser intensity. It is important to note, that temporal spreading, spatial distortion, and absorption are all minimised for light-pulse propagation under ultra-slow light conditions because of the linear variation of the refractive index with frequency around its unity value at resonance.

The dramatic spatial pulse compression and coherent, holographic imprinting of optical information in atomic media, associated with ultra-slow light, led to the observation of stopped light. Using this technique, we envision developing three-dimensional optical storage devices with optical information stored in highly compressed form, and the creation of optical shift registers controlled by the on/off switching of a coupling laser with illumination in spatially selected regions. Dynamical bandwidth control for transform limited pulse propagation is possible, as is controlled coherent processing of optical information through utilisation of the coherent dynamics of Bose-Einstein condensates. Furthermore, ultra-slow-light-based output-coupling from condensates of very localised coherent structures with controlled spatial shapes and recoil

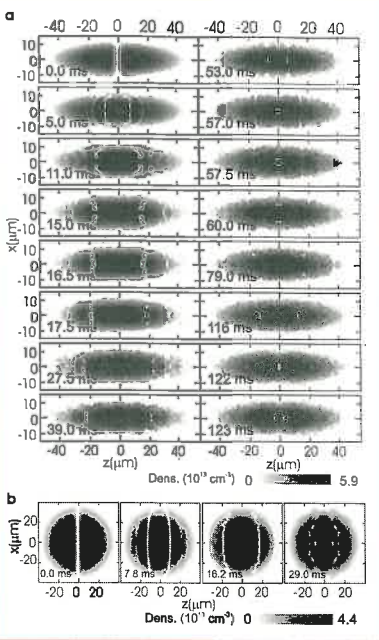


**Fig. 6: Quantum Shock Waves and Vortex Dynamics**
**(a)** Vortex dynamics. A numerical calculation of the dynamics for a sodium condensate after a deep, narrow density defect has been created at *t=0* at a light roadblock. The dynamics are calculated with the non-linear Gross-Pitaevskii equation [12], and the plots show the density of the condensate at the times indicated. The formation, dynamics, and interactions of the vortices formed by the defect are discussed in the text. The size and amplitude of the defect is controlled with the duration and intensity of the probe pulse and in this case, a 100 % density defect, with a half-width of 3 μm, is imposed initially, and this leads to formation of 4 long-lived vortices that first collide like billiard balls (at 57 ms) and then scatter off the condensate boundaries. A second collision (at 122 ms) results in the creation of a large spherically outgoing sound wave (123 ms).
**(b)** Many-body system of vortices. Numerical calculation of the dynamics for a condensate, trapped in a spherically symmetric magnetic field, after a defect with half-width 2.3 μm is imposed. We see that the deepest solitons break up into ten vortices each. The number of vortices formed is determined by the intensity and duration of the probe pulse, and the light roadblock is therefore ideal for controlled studies of many-body systems of vortices.

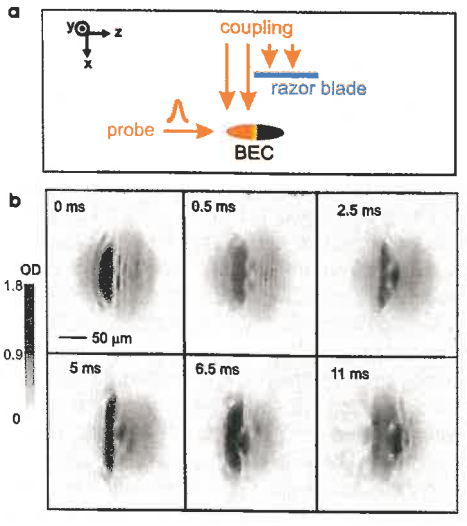


**Fig. 5: Light Roadblock and Quantum Shock Waves in Bose-Einstein Condensates**
**(a)** Light roadblock. A razor blade blocks the coupling beam from illuminating the far (*z>0*) side of the condensate. When the slowed probe light pulse reaches the roadblock (at *z=0*), where the coupling intensity drops to zero, the light pulse is further slowed and dramatically compressed to only a few microns, creating a narrow imprint of $|2\rangle$ atoms in the condensate. This imprint is kicked out (as in Fig. 2) and leaves a condensate of state $|1\rangle$ atoms trapped in the magnet, with a narrow density depletion in the middle. The narrow defect results in the formation of two density dips that propagate at the sound speed towards the condensate boundaries. Due to the dramatic variation of atom density and local sound speed across the structures, the back parts of the dips will catch up to the central parts, and the back edges will steepen. This process would in a normal fluid lead to shock wave formation. Here, where we form the defects in a Bose-Einstein condensate, we create the superfluid analogues of shock waves, 'quantum shock waves', in the form of topological defects (for example, dark solitons).
**(b)** Observation of quantum shock waves at the light roadblock (from ref. 10). After the density defect is formed at the light roadblock, we leave the condensate of $|1\rangle$ atoms trapped in the magnet for a varying amount of time (as indicated in the figures). We then abruptly turn the trap off and let the cloud expand for 15 ms. We subsequently image the central slice of the dropping condensate with the imaging beam (Fig. 1a) (the vertical height (along *y*) of the slice is 30 μm). We immediately observe (at 0 ms) the appearance of a series of white stripes (white means no condensate density), which indicate that dark solitons have been formed. The solitons are unstable, and the fronts are observed to curve after just 0.5 ms ('snake instability' [31]). The points along the main front, with large curvature, act as nucleation sites for quantized vortices, and at 2.5 ms we observe that two vortices have formed (seen as white dots in the figure). These two vortices are very stable, and they are clearly seen at 11 ms, for example. In the process, the overall shape of the condensate is also changing dramatically (indicating the presence of a large collective excitation of the condensate). At 5 ms the condensate is long, dense, and narrow. The condensate subsequently relaxes into the extended shape seen at 11 ms.

momenta could be of great importance for atom-interferometry.

Ultra-slow light also allows for extreme optics. Nonlinear optical effects associated with slow light are so large [1,29]—due to the steep refractive index profile—that nonlinear optics close to the single photon level is possible with micron-sized structures. For example, ultra-sensitive switches, with a switching energy corresponding to just two photons ($10^{-18}$ Joule), and frequency up-conversion at very low power levels are possible.

With use of the light roadblock, light pulses have been compressed to sizes comparable to the wavelength of light, a very interesting regime for further studies. Furthermore, creation of vortices at the light roadblock makes possible unprecedented and direct studies of vortex collision dynamics in superfluids. Superfluidity is a property which allows BECs to flow without dissipation, and equivalently, superconductors to conduct currents with no resistance. Vortex collisions are expected to form the main mechanism by which dissipation is introduced into superfluid systems and are therefore of fundamental importance for understanding the breakdown of superfluidity and superconductivity.

## Acknowledgement

The research was supported by the U.S. Airforce Office of Scientific Research, the U.S. Army Research Office OSD Multidisciplinary University Research Initiative Program, The National Science Foundation, and the National Aeronautics and Space Administration. CS was supported by a National Defense Science and Engineering Fellowship sponsored by the U.S. Department of Defense.

## About the author

Lene Vestergaard Hau is Gordon McKay Professor of Applied Physics and Professor of Physics at Harvard University. She received her Ph.D. from the University of Aarhus, Denmark. She was named MacArthur Fellow in 2001 and just received the 2004 Richtmyer Memorial Lecture Award.

## References

[1] Hau, L.V., Harris, S.E., Dutton, Z., and Behroozi, C.H., Light speed reduction to 17 metres per second in an ultracold atomic gas. *Nature* **397**, 594-598 (1999).

[2] Inguscio, M., Stringary, S., and Wieman, C., eds., Bose-Einstein Condensation in Aomtic Gases, *Proceedings of the International School of Physics Enrico Fermi, Course CXL*, (International Organisations Services, Amsterdam, 1999).

[3] Hau, L.V. Bose-Einstein condensation and light speeds of 38 miles/hour, in proceedings from the Workshop on Bose-Einstein Condensation and Degenerate Fermi Gases, Feb. 10-12, 1999 (Centre for Theoretical Atomic, Molecular, and Optical Physics, Boulder, CO) http://fermion.colorado.edu/~chg/Talks/Hau

[4] Liu, C., Dutton, Z., Behroozi, C.H., and Hau, L.V., Observation of coherent optical information storage in an atomic medium using halted light pulses. *Nature* **409**, 490-493 (2001).

[5] Kash, M.M., *et al.*, Ultraslow group velocity and enhanced nonlinear optical effects in a coherently driven hot atomic gas. *Phys. Rev. Lett.* **82**, 5229-5232 (1999).

[6] Budker, D., Kimball, D.F., Rochester, S.M., Yashchuk, V.V., Nonlinear magneto-optics and reduced group velocity of light in atomic vapour with slow ground state relaxation. *Phys. Rev. Lett.* **83**, 1767-1770 (1999).

[7] Phillips D.F., Fleischhauer, A., Mair, A., Walsworth, R.L., and Lukin, M.D., Storage of light in atomic vapour. *Phys. Rev. Lett.* **86**, 783-786 (2001).

[8] Turukhin, A.V., *et al.*, Observation of ultraslow and stored light pulses in a solid. *Phys. Rev. Lett.* **88**, 023602 (2002).

[9] Bigelow, M.S., Lepeshkin, N.N., and Boyd, R.W., Observation of Ultraslow Light Propagation in a Ruby Crystal at Room Temperature. *Phys. Rev. Lett.* 90, 113903-1 (2003).

[10] Dutton, Z., Budde, M., Slowe, C., and Hau, L.V., Observation of quantum shock waves created with ultra-compressed slow light pulses in a Bose-Einstein Condensate. *Science* **293**, 663-668 (2001).

[11] Harris, S.E., Electromagnetically induced transparency. *Physics Today* **50**, 36-42 (1997).

[12] Dalfovo , F., Giorgini, G., Pitaevskii , L.P., and Stringari , S., Theory of Bose-Einstein condensation in trapped gases. *Rev. Mod. Phys.* **71**, 463–512 (1999).

[13] Gustavson, T. L., Landragin, A., Kasevich, M. A., Rotation sensing with a dual atom-interferometer Sagnac gyroscope. *Classical Quant. Grav.* **17**, 2385-2398 (2000).

[14] Snadden, M. J., McGuirk, J. M., Bouyer, P., Haritos, K. G., Kasevich, M. A., Measurement of the earth's gravity gradient with an atom interferometer-based gravity gradiometer. Phys. Rev. Lett. **81**, 971-974 (1998); Peters, A., Chung, K. Y., Chu, S., Measurement of gravitational acceleration by dropping atoms. *Nature* **400**, 849-852 (1999).

[15] Dutton, Z. and Hau, L.V., in preparation.

[16] Dutton, Z., Ph.D. Thesis, (Harvard University, 2002).

[17] Burger, S., Bongs, K., Dettmer, S., Ertmer, W., and Sengstock, K., Dark Solitons in Bose-Einstein Condensates. *Phys. Rev. Lett.* **83**, 5198–5201 (1999).

[18] Manakov, S.V., On the theory of two-dimensional stationary self-focusing of electromagnetic waves. Soviet Phys. *JETP* **38**, 248-253 (1974).

[19] Busch, T., Anglin, J.R., Dark-bright solitons in inhomogeneous Bose-Einstein condensates. *Phys Rev. Lett.* **87**, 010401 (2001).

[20] Inouye, S., *et al.*, Observation of Feshbach resonances in a Bose-Einstein condensate. *Nature* **392**,151-154 (1998).

[21] Cornish, S.L., Claussen, N.R., Roberts, J.L., Cornell, E.A., and Wieman, C.E., Stable Rb-85 Bose-Einstein condensates with widely tunable interactions. *Phys. Rev. Lett.* **85**, 1795-1798 (2000).

[22] M. Kitagawa and M. Ueda, Squeezed spin states. *Phys. Rev. A* **47**, 5138–5143 (1993).

[23] Sorensen, A., Duan, L.-M., Cirac, J.I., and Zoller, P., Many-particle entanglement with Bose-Einstein condensates. *Nature* **409**, 63-66 (2001).

[24] Lukin, M.D., Yelin, S.F., and Fleischhauer, M., Entanglement of atomic ensembles by trapping correlated photon states. *Phys. Rev. Lett.* **84**, 4232-3235 (2000).

[25] DiVincenzo, D.P., The physical implementation of quantum computation, *Fortsch. Phys.* **48**, 771-783 (2000).

[26] Donnelly, R.J., *Quantized vortices in Helium II*, (Cambridge Univ. Press, Cambridge, 1991).

[27] Leonhardt, U., A laboratory analogue of the event horizon using slow light in an atomic medium, *Nature* **415**, 406 (2002).

[28] Bajcsy, M., Zibrov, A. S., Lukin, M. D., Stationary pulses of light in an atomic medium, *Nature* **426**, 638 (2003).

[29] Harris, S.E. and Hau, L.V., Nonlinear optics at low light levels, *Phys. Rev. Lett.*, **82**, 4611 (1999).

[30] Myatt, C.J., Burt, E.A., Ghrist, R.W., Cornell, E.A., and Wieman, C.E., Production of Two Overlapping Bose-Einstein Condensates by Sympathetic Cooling. *Phys. Rev. Lett.* **78**, 586-589 (1997).

[31] Anderson, B.P., *et al.*, Watching dark solitons decay into vortex rings in a Bose-Einstein condensate. *Phys. Rev. Lett.* **86**, 2926-2929 (2001).